Optica Applicata, Vol. XXXVII, No. 4, 2007

Crystallization kinetics of $Fe_{78}Si_9B_{13}$ metallic glass

E. JAKUBCZYK[1*], L. KRAJCZYK[2], P. SIEMION[3], M. JAKUBCZYK[3]

[1]Institute of Physics, Jan Długosz University, al. Armii Krajowej 13/15, 42-200 Częstochowa, Poland

[2]Institute of Low Temperature and Structure Research, Polish Academy of Sciences, Okólna 2, 50-950 Wrocław, Poland

[3]Institute of Chemistry and Environmental Protection, Jan Długosz University, al. Armii Krajowej 13/15, 42-200 Częstochowa, Poland

[*]Corresponding author: e.jakubczyk@ajd.czest.pl

The investigation of $Fe_{78}Si_9B_{13}$ metallic glass was carried out by means of non-isothermal DSC and X-ray diffraction methods. Two crystalline phases: α-Fe(Si) and $(Fe,Si)_2B$ were identified during the crystallization process. Based on the Kissinger equation the activation energies for both phases were calculated. Using the Gao equation the Avrami kinetics exponent was determined. TEM studies proved the creation of these phases and also showed the presence of the FeB_{49} phase in the remaining amorphous phase.

Keywords: metallic glass, non-isothermal crystallization, activation energy, kinetics exponent.

1. Introduction

The structure of as-received metallic glasses is not in thermodynamic equilibrium and spontaneously evolves to new more stable structures, often through intermediate metastable phases. Structural modifications cause changes in the short and medium range order and finally lead to a stable polycrystalline state, in which a long range order is seen. These structural changes cause modifications of the physical properties [1, 2]. Crystallization studies of metallic glasses are interesting from many points of view. The results of such studies are helpful in understanding the mechanism and kinetics of phase transformation into the equilibrium state. They also allow us to evaluate the glass forming ability from the melt and predict stability of the amorphous state. Moreover, the crystallization studies make a controlled production of micro- and nano-structures possible.

Theoretical description of the crystallization kinetics of metallic glasses is possible using appropriate kinetics equations containing characteristic parameters [3, 4]. The glass-crystal transformation may be studied experimentally using isothermal or

non-isothermal analysis techniques. The isothermal analysis methods are more definitive, but non-isothermal ones have still some advantages, *i.e.*, the rate at which the experiment can be performed and the extended temperature range that can be used during the measurements. The non-isothermal methods allow us to use equipment with not so defined accuracy [5].

This paper is a continuation of the investigation of the crystallization process of $Fe_{78}Si_9B_{13}$ metallic glass [6, 7]. The results of X-ray diffraction (XRD) presented in those papers proved creation of the stable crystalline phases: α-Fe(Si) and $(Fe,Si)_2B$ at different temperatures. Based on the results of differential scanning calorimetry (DSC) measurements, the activation energy corresponding to the formation of these phases was calculated. The total energy of clusters representing these phases was calculated by quantum chemistry methods. The measurements of Hall and electrical resistivities proved the influence of the structural changes on the electrical properties of the alloy. Particularly, a distinct decrease of these values was observed after formation of the stable crystalline phases.

The amorphous alloys based on Fe–Si–B are successfully applied as the core materials in distribution transformers, due to their low core losses and relatively high saturation magnetization [8]. Therefore, it is necessary to determine both the conditions in which the properties of as-received state of metallic glasses are conserved and the parameters of the kinetics of structure transformations.

The aim of this study is to analyse the kinetics of crystallization of $Fe_{78}Si_9B_{13}$ metallic glass through DSC and X-ray and transmission electron microscopy (TEM) techniques. In particular, the Avrami kinetics exponents were determined and the phases created as well as their structure and morphology were idendified.

2. Experimental

The metallic glass $Fe_{78}Si_9B_{13}$ was prepared by the roller quenching method in the Institute of Materials Engineering of the Warsaw Technical University, Poland.

DSC measurements were carried out using an STA-409 NETZSCH apparatus under continuous heating. The heating rates were 5, 10, 15 and 20 K/min. The scanning temperature varied from room temperature up to 900 K, with the accuracy of ±0.1 K. High purity argon was used as inert atmosphere. The mass of the sample was typically 22–25 mg.

The XRD studies were carried out at room temperature for the as-received as well as isochronally (4 h) annealed samples at various temperatures (573–823 K) and also for samples isothermally annealed at 673 K for different times ($\leq 2\times10^4$ s). Use was made of a DRON-2.0 diffractometer with a horizontal goniometer of GUR-5 type. The XRD tube had a molybdenium target ($\lambda_{K\alpha} = 0.71069\times10^{-10}$ m) and a graphite monochromator in the primary beam.

High resolution transmission electron microscopy (HRTEM) and selected area electron diffraction (SAED) studies were performed using a 200 kV Philips Super-Twin microscope providing 0.24 nm resolution. For HRTEM measurements fine powder

samples were prepared by grinding the samples in mortar and dispersing in methanol with ultrasonic agitation. A droplet of suspension was deposited on a microscope grid covered with holey carbon film.

3. Résumé of nucleation and growth kinetics

A newly created phase does not need to be always the thermodynamically most stable one. When the thermodynamically stable crystals nucleate and grow directly from the parent phase, it is a one-stage process of the crystallization (path 1 in Fig. 1). In the case where the formation of the stable crystalline phase is not direct, but it is carried through metastable phases, the crystallization is a two- or multi-stage process (path 2 in Fig. 1) [9]. A physical picture of the two stages of the crystallization process is presented in Fig. 2 [9, 10]. The volume fractions of the metastable $x_m(t)$ and stable crystalline phases $x_s(t)$ at the time t are defined as:

$$x_m(t) = \frac{V_m(t)}{V} \qquad x_s(t) = \frac{V_s(t)}{V} \tag{1}$$

where V_m, V_s, V are the total volumes of metastable, crystalline and parent phases, respectively.

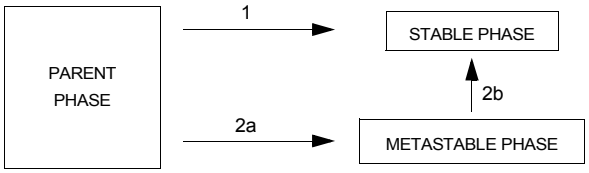

Fig. 1. One-stage (path 1) and two-stage (paths 2a–2b) formation of stable phase [9].

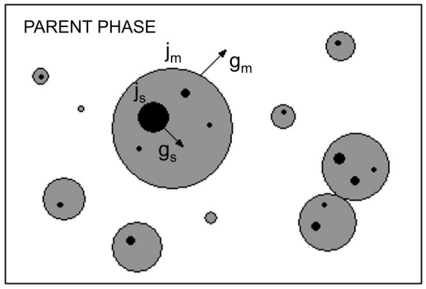

Fig. 2. Scheme of two-stage of crystallization process (j_m, j_s and g_m, g_s are nucleation and growth rates of metastable phase – grey circles and stable phase – black circles) [9, 10].

According to the Kolmogorov, Johnson, Mehl and Avrami (KJMA) theory, the time dependence of the volume fraction $x(t)$ for the isomorphic growing particles within the matrix is given by [9, 10]:

$$x(t) = 1 - \exp\left\{-c\int_0^t j(t')\left[\int_{t'}^t g(\tau - t')\mathrm{d}\tau\right]^d \mathrm{d}t'\right\} \tag{2}$$

where: d is the dimensionality of the particles (d = 1, 2 and 3 for needle-, disk-, and sphere-like, respectively), c is the shape factor, j and g are the nucleation and growth rates of the particles (Fig. 2). The KJMA formula shows explicitly that the evolution of the fraction of crystallized volume is controlled by the nucleation and growth of the crystallites. The polynuclear mechanism is characteristic of the multicomponent amorphous alloys and it has two distinct manifestations known as instantaneous and progressive nucleation. When all crystallites in the system are nucleated simultaneously at the initial moment the nucleation is instantaneous and described by the equation:

$$j(t) = \frac{N_m}{V}\delta_D(t) \tag{3}$$

where: N_m – the maximum number of crystallites, δ_D – the Dirac delta function [10].

In the case of the progressive nucleation the crystallites are continuously nucleated during the process. In order to simplify the analysis of this process the nucleation is often taken as stationary:

$$j_s = A\exp\left(-\frac{W^*}{kT}\right) \tag{4}$$

where: W^* is the work necessary for nucleus formation, k is the Boltzmann constant and A is a kinetic parameter in stationary nucleation rate.

According to the time dependence given by the unified KJMA formula the volume fraction of the metastable phase is:

$$x_m(t) = 1 - \exp\left[-(K_m t)^m\right] \tag{5}$$

where m and K_m are the kinetic exponent and the reaction rate constant characterizing the metastable phase [10].

A stable crystalline phase is formed within the variable volume metastable phase, and those two often have different kinetics. Therefore, in order to determine a volume of the stable crystalline phase formed, a differential form of the equation analogous to (5) must be used. If t' is an initial moment of the crystallization process of the stable phase in the volume $\mathrm{d}V_m$, the volume stable phase $\mathrm{d}V_s$ may be written as [9, 10]:

$$\mathrm{d}V_s = \left\{1 - \exp\left[-\left(K_s(t - t')\right)^s\right]\right\}\mathrm{d}V_m \tag{6}$$

Integrating this equation in limits: $t' = 0$ to $t' = t$ and $V_s = 0$ to $V_s = V_s(t)$ and dividing by V leads to the general formula for the volume fraction of the stable crystalline phase x_s

$$x_s(t) = x_m(t) - \int_0^t \exp\left\{-\left[K_s(t-t')\right]^s\right\}\left[\frac{\mathrm{d}x_m(t')}{\mathrm{d}t'}\right]\mathrm{d}t' \tag{7}$$

The above equation shows that x_s depends on both the kinetics of appearance of the stable phase (*i.e.*, on the kinetic exponent s and on the reaction rate constant K_s) and the rate $\mathrm{d}x_m/\mathrm{d}t$ of the metastable phase formation.

The reaction rate constants K_m or K_s for the stationary nucleation and power-law growth of particles according to the KJMA kinetics are described by the following equations [9]:

$$K_m = \left(\frac{c_m j_m g_m^{n-1}}{n}\right)^{1/n} \tag{8a}$$

$$K_s = \left(\frac{c_s j_s g_s^{n-1}}{n}\right)^{1/n} \tag{8b}$$

where $n = 1 + \nu d$, (ν is specified as 0.5 and 1 for parabolic and linear growths, respectively) [9].

In the case of stationary nucleation and three-dimensional growth ($d = 3$) of crystallites with the time-independent growth rate ($\nu = 1$), the kinetic exponent $n = 4$. Kashchiev and Sato transformed Eq. (7) to the analytical form (for $K_m t \geq b'$, where $b' \equiv (m - 1/m)^{1/m}$) which leads to a simple formula for the time dependence of the volume fraction of the metastable phase into the stable crystalline one [9, 10]:

$$x_s(t) = x_m(t)\left\{1 - \exp\left[-\left(\frac{K_s}{K_m}\right)^s\left(K_m t - b'\right)^s\right]\right\} \tag{9}$$

The numerical calculation proves that the time at which x_s starts departing appreciably from zero is controlled by the value of the ratio K_s/K_m between the reaction rate constants of both phases formed in two-stage crystallization [10]. When the value of K_s/K_m ratio is small the formation of the stable crystalline phase is delayed. This delay can be so long that the first portion of the stable phase appears after the complete formation of the metastable phase. For large K_s/K_m values $x_s(t)$ is close to $x_m(t)$ (and at $K_s/K_m = \infty$ gives $x_s(t) = x_m(t)$). In this case, the metastable phase (according to Ostwald's rule of stages), transforms into the stable crystalline phase so quickly that it may not be experimentally observable when the applied technique is of low resolution [9].

4. Theoretical basis of non-isothermal treatment

The isothermal solid state transformations are strictly described by the KJMA equation of general form:

$$x(t) = 1 - \exp\left[-(Kt)^n\right] \tag{10}$$

where x is the volume fraction transformed at time t, n – a dimensionless quantity called the kinetic exponent, and K – the reaction rate constant. The temperature dependence of K is generally expressed by the Arrhenius equation:

$$K(T) = K_0 \exp\left(-\frac{E_a}{RT}\right) \tag{11}$$

Differentiating Eq. (10) with respect to t at constant temperature gives the reaction rate $\mathrm{d}x/\mathrm{d}t$:

$$\frac{\mathrm{d}x}{\mathrm{d}t} = n K^n t^{n-1}(1-x) = nK(1-x)\left[-\ln(1-x)\right]^{\frac{n-1}{n}} \tag{12}$$

The rates of crystallization $\mathrm{d}x/\mathrm{d}t$ at various times are measured directly in the case of isothermal DSC experiment. The double logarithm of Eq. (10) leads to:

$$\ln\left[-\ln(1-x)\right] = n\ln K + n\ln t \tag{13}$$

and then values of n and K are determined from expression (13) by the least-squares fitting of $\ln[-\ln(1-x)]$ versus $\ln t$. Next, the activation energy E_a and the frequency factor K_0 can be evaluated from the logarithmic form of Eq. (11).

However, it is very interesting to generalize the KJMA equation to experiments in which the rate of heating $\beta = \mathrm{d}T/\mathrm{d}t$ is constant. In order to determine maximum of the crystallization rate the second derivative of Eq. (10) was calculated giving [11]:

$$\frac{\mathrm{d}^2x}{\mathrm{d}t^2} = \beta\left[\frac{\mathrm{d}(\ln K)}{\mathrm{d}T}\right]\left(\frac{\mathrm{d}x}{\mathrm{d}t}\right) + (nK)\frac{\mathrm{d}\left\{(1-x)\left[-\ln(1-x)\right]^{\frac{n-1}{n}}\right\}}{\mathrm{d}x}\left(\frac{\mathrm{d}x}{\mathrm{d}t}\right) = 0 \tag{14}$$

Substituting the result of differentiation of Eq. (11):

$$\frac{\mathrm{d}(\ln K)}{\mathrm{d}t} = \frac{E_a}{RT^2} \tag{15}$$

into (14) and next integrating the equation obtained within limits: 0 to x_p and 0 to T_p one can obtain:

$$\left[-\ln(1-x_p)\right]^{1/n} = \frac{K_0 T_p}{\beta} E_2\left(\frac{E_a}{RT_p}\right) \tag{16}$$

where subscript p stands for the magnitudes at the maximum crystallization rate, E_2 and Y are given by relations:

$$E_2\left(\frac{E_a}{RT_p}\right) = \frac{\exp(-E_a/RT_p)}{E_a/RT_p + 2}(1 + Y)$$

$$Y = 2\left(\frac{E_a}{RT_p} + 2\right)^{-2} + \text{terms of higher order}$$

In the crystallization process $Y \ll 1$, because $E_a \gg RT_p$. Combining Eqs. (16) and (11) (at the maximum crystallization rate) leads to [11]:

$$\left[-\ln(1 - x_p)\right]^{-1/n} = \frac{\beta E_a(1 + 2RT_p/E_a)}{K_p R T_p^2} \approx \frac{\beta E_a}{K_p R T_p^2} \tag{17}$$

Using Eqs. (14) and (17) yields:

$$\frac{\beta E_a}{K_p R T_p^2} = 1 \tag{18}$$

and Eqs. (17) and (18) lead to: $-\ln(1 - x_p) = 1$ and hence $x_p = 0.63$.

Substituting this value of x_p for x in Eq. (12) gives the kinetics exponent n of the crystallization:

$$n = \left(\frac{\mathrm{d}x}{\mathrm{d}t}\right)_p RT_p^2\left(0.37\beta E_a\right)^{-1} \tag{19}$$

Although the KJMA equation was deduced for the isothermal case, it is widely applied also by many authors to the non-isothermal crystallization process [11–13]. The KJMA equation is used in a variety of mathematical analysis of the non-isothermal solid state transformation.

5. Results and discussion

The kinetics of non-isothermal crystallization of $Fe_{78}Si_9B_{13}$ metallic glass was investigated by DSC method. The measurements were carried out at continuous heating rates of 5, 10, 15 and 20 K/min. In each DSC curve two clearly separated exothermic peaks are seen. This indicates that during the transformations two principal crystalline phases appear. The position of the peaks on the temperature axis moves towards the higher temperature with an increase of the heating rate. Based on the Kissinger equation the activation energy E_a for the crystallized phases can be derived from:

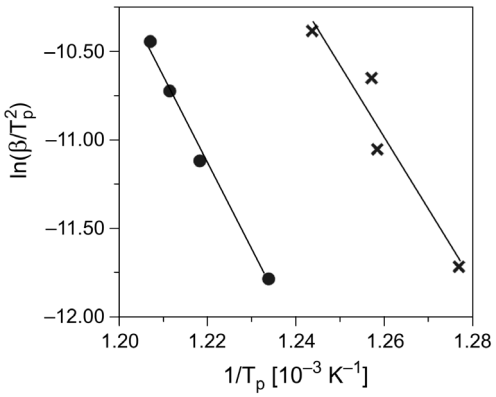

Fig. 3. Dependences of $\ln(\beta/T_p^2)$ versus $1/T_p$ for both stages of crystallization of $Fe_{78}Si_9B_{13}$ metallic glass (● – first stage and × – second stage).

$$\ln\left(\frac{\beta}{T_p^2}\right) = -\frac{E_a}{RT_p} + \ln\left(\frac{K_0 R}{E_a}\right) \tag{20}$$

where: $\beta = \mathrm{d}T/\mathrm{d}t$ is the heating rate, T_p temperature of the peak, R the gas constant and K_0 frequency factor [14, 15]. The Kissinger plots, that is $\ln(\beta/T_p^2)$ vs. $1/T_p$ (Fig. 3), allow the values of E_a to be obtained through the least-squares fit. The calculated values of are listed in the Table.

T a b l e. Parameters of crystallization kinetics of $Fe_{78}Si_9B_{13}$ metallic glass.

Parameter	α-Fe(Si)	$(Fe,Si)_2B$
E_a [kJ/mol]	341	410
n	2.49	4.93

Here, we calculated the Avrami kinetics exponent n from Eq. (19) developed for the first time by GAO and WANG [11]. The crystallized fraction x at any temperature T is given as $x = A_x/A$, where A and A_x are the total and partial (at generic temperature T) areas of exothermic peak, respectively. The crystallization rates vs. temperature for the two principal crystalline phases observed are presented in Figs. 4 and 5. The maximum crystallization $(\mathrm{d}x/\mathrm{d}t)_p$ for each heating rate gives n according to Eq. (19). The average values n for both phases are included in the Table. They indicate that the crystalline grains of both phases are three-dimensional [9].

Figure 6 presents the results of X-ray diffraction. They also prove that in the crystallization process there are two crystalline phases formed at different temperatures. A qualitative analysis proves that the cubic α-Fe(Si) phase ($Im\bar{3}m$; $a = 2.856$ Å) is created at 723 K and the tetragonal $(Fe,Si)_2B$ phase (I4/mcm; $a = 5.105$ Å, $b = 4.228$ Å) appears after annealing at 773 K [16, 17]. The isothermal

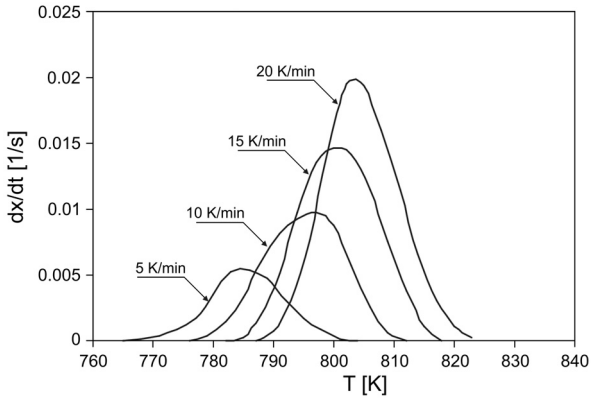

Fig. 4. Crystallization rate dx/dt versus temperature T for the $Fe_{78}Si_9B_{13}$ metallic glass at different heating rates for the first crystalline phase.

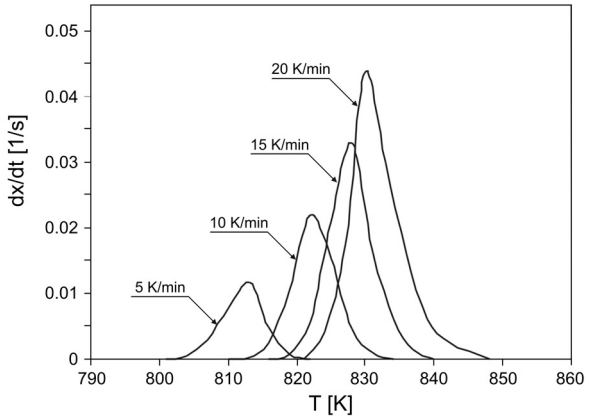

Fig. 5. Crystallization rate dx/dt versus temperature T for the $Fe_{78}Si_9B_{13}$ metallic glass at different heating rates for the second crystalline phase.

annealing at 673 K indicates that the crystallization process starts after annealing time $\tau \geq 2\times10^4$ s (Fig. 6**b**). The as-received metallic glass is amorphous and homogenous (Figs. 6**a** and 6**b**), thus the volume diffusion of Fe atoms causes the formation of the metastable Fe(Si) phase in some areas of the parent phase. These areas transform to the crystalline α-Fe(Si) phase after annealing at a temperature of 723 K. Such a phase transition is the primary crystallization [18, 19]. The chemical composition and the properties of the amorphous matrix change during the primary crystallization. As a result of this process the amorphous matrix phase enriches in boron atoms and attains the eutectic composition: α-Fe(Si) + $(Fe,Si)_2B$. As the annealing temperature increases further and reaches the point (773 K) of the eutectic reaction occurs.

The TEM and SAED studies of $Fe_{78}Si_9B_{13}$ specimen heated at 823 K for 4 h verify the creation of the phases discussed above on the basis of XRD measurements.

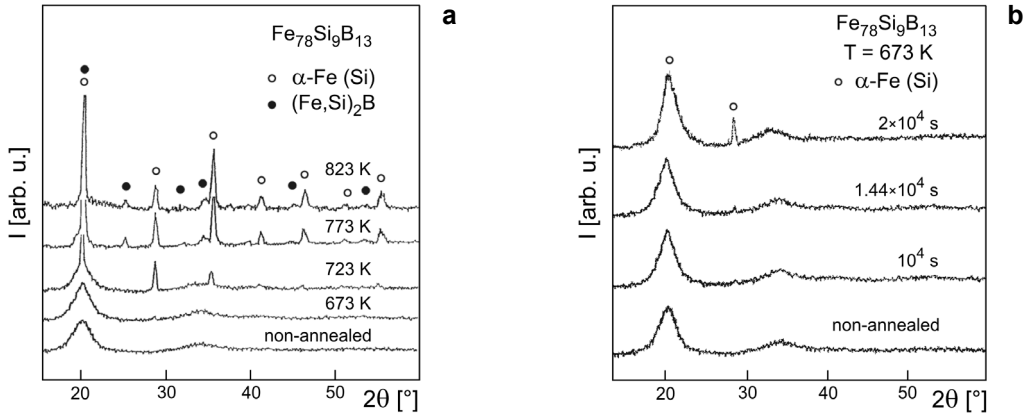

Fig. 6. X-ray diffraction patterns for samples of the alloy $Fe_{78}Si_9B_{13}$ annealed: at different temperatures (**a**), during different time intervals at 673 K (**b**).

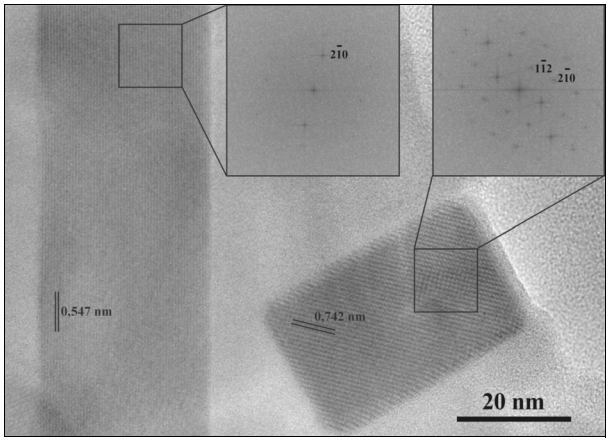

Fig. 7. HRTEM image and its Fourier transforms of specimen $Fe_{78}Si_9B_{13}$ heated at 823 K for 4 h. Particles with 0.742 and 0.547 nm latice fringes characteristic of $[1\bar{1}2]$ and $[2\bar{1}0]$ of FeB_{49} are visible.

However, some amount of the amorphous phase was also observed following the applied treatment of the specimen (Fig. 7). Additionally, TEM observations showed the presence of a needle-like cuboid shaped large crystalline particles, typically between 20 and 50 nm in shorter, and even up to 500 nm in elongated sizes. A magnified image of such crystallites is shown in Fig. 7 with its fast Fourier transform (FFT). The phase analysis of them was carried out by indexing the selected area diffraction patterns as well as the FFT patterns obtained from the HRTEM image of the nanocrystalline particles [20, 21]. The analysis results indicate that the particles with 0.742 and 0.547 lattice fringes are characteristic of $[1\bar{1}2]$ and $[2\bar{1}0]$, respectively, of the FeB_{49} compound [22]. Thus, the FeB_{49} phase, very rich in boron, was identified in the sample under study.

6. Conclusions

The following conclusions can be derived from conducted studies:

1. DSC and XRD studies indicate that the transformation from the amorphous to crystalline state proceeds through the formation of two main stable phases: α-Fe(Si) and $(Fe,Si)_2B$.

2. The high resolution and electron diffraction observations show that after annealing at 823 K for 4 h some part of the amorphous phase is still present in the volume of specimen.

3. By means of TEM techniques the presence of the FeB_{49} phase was detected.

4. The values of the Avrami kinetics exponents indicate that the phases formed grow as the three-dimensional crystals.

References

[1] KOMATSU T., *Structural relaxation and related processes in metallic glasses*, Res Mechanica **31**(3), 1990, pp. 263–83.

[2] JAKUBCZYK E., JAKUBCZYK M., *Changes of properties during the annealing $Fe_{28}Co_{50}Si_9B_{13}$ and $Fe_{28}Ni_{50}Si_9B_{13}$ metallic glasses*, Optica Applicata **32**(3), 2002, pp. 241–6.

[3] CHRISTIAN J.W., *The Theory of Transformation in Metals and Alloys*, Pergamon Press, Oxford 1965.

[4] HENDERSON D.W., *Thermal analysis of non-isothermal crystallization kinetics in glass forming liquids*, Journal of Non-Crystalline Solids **30**(3), 1979, pp. 301–15.

[5] VÁZQUEZ J, LÓPEZ-ALEMANY P.L.,.VILLARES P, JIMÉNEZ-GARAY R., *Generalization of the Avrami equation for the analysis of non-isothermal transformation kinetics. Application to the crystallization of the $Cu_{0.20}As_{0.30}Se_{0.50}$ alloy*, Journal of the Physics and Chemistry of Solids **61**(4), 2000, pp. 493–500.

[6] JAKUBCZYK E., STĘPIEŃ Z., JAKUBCZYK M., *Influence of the composition of $M_{78}Si_9B_{13}$ metallic glasses on their structural stability*, Optica Applicata **35**(3), 2005, pp. 339–46.

[7] JAKUBCZYK E., *Phase transitions in $Co_{78}Si_9B_{13}$ and $Fe_{78}Si_9B_{13}$ metallic glasses induced by isochronal annealing*, Materials Science Poland **24**(4), 2006, pp. 1027–36.

[8] HASEGAWA R., *Applications of amorphous magnetic alloys*, Materials Science and Engineering A **A375–377**, 2004, pp. 90–7.

[9] KASHCHIEV D., SATO K., *Kinetics of crystallization preceded by metastable-phase formation*, Journal of Chemical Physics **109**(19), 1998, pp. 8530–40.

[10] KASHCHIEV D., *Nucleation: Basic Theory with Applications*, Butterworth-Heinemann, Oxford 2003.

[11] GAO Y.Q., WANG W., *On the activation energy of crystallization in metallic glasses*, Journal of Non-Crystalline Solids **81**(1–2), 1986, pp. 129 –34.

[12] VÁZQUEZ J, LÓPEZ-ALEMANY P.L., VILLARES P, JIMÉNEZ-GARAY R., *A study on non-isothermal transformation kinetics. Application to the crystallization of $Sb_{0.20}As_{0.32}Se_{0.48}$ alloy*, Journal of Alloys and Compounds **270**(1–2), 1998, pp. 179–85.

[13] OZAWA T., *Kinetics of non-isothermal crystallization*, Polymer **12**(3), 1971, pp. 150–8.

[14] KISSINGER H.E., *Reaction kinetics in differential thermal analysis*, Analytical Chemistry **29**(11), 1957, pp. 1702–6.

[15] LIU L., CHAN K.C., *Amorphous-to-quasicrystalline transformation in $Zr_{65}Ni_{10}Cu_{7.5}Al_{7.5}Ag_{10}$ bulk metallic glass*, Journal of Alloys and Compounds **364**, 2004, pp. 146–55.

[16] TOMASZEWSKI P.E., *Golden Book of Phase Transitions*, Wrocław 2002.

[17] HAVINGA E.E., DAMSMA H., HOKKELING P., *Compounds and pseudo-binary alloys with the $CuAl_2$ (C16)- type structure., I. Preparation and X-ray results*, Journal of the Less Common Metals **27**(2), 1972, pp. 169–86.

[18] KÖSTER U., *Phase transformations in rapidly solidified alloys*, Key Engineering Materials **81–83**, 1993, pp. 647–62.
[19] KIM C.K., *Effects of crystallization on the coercivity in $Fe_{78}Si_9B_{13}$ amorphous alloy*, Materials Science and Engineering B **B39**(3), 1996, pp. 195–201.
[20] SPENCE J.C.H., *High Resolution Electon Microscopy*, Ed. 3, Oxford University Press, New York 2003.
[21] AMELINCKX S., GEVERSR., VAN LANDUYT J., *Diffraction and Imaging Techniques in Material Science*, Nort-Holland Publishing Company, Amsterdam, New York, Oxford 1979.
[22] CALLMER B., LUNDSTROEM T., *A single-crystal diffractometry investigation of iron in beta-rhombohedral boron*, Journal of Solid State Chemistry **17**(1–2), 1976, pp. 165–70.

Received May 14, 2007
in revised form October 11, 2007